

# Na<sub>2</sub>IrO<sub>3</sub> as a molecular orbital crystal

I. I. Mazin,<sup>1</sup> Harald O. Jeschke,<sup>2</sup> Kateryna Foyevtsova,<sup>2</sup> Roser Valentí,<sup>2</sup> and D. I. Khomskii<sup>3</sup>

<sup>1</sup>Code 6393, Naval Research Laboratory, Washington, DC 20375, USA

<sup>2</sup>Institut für Theoretische Physik, Goethe-Universität Frankfurt, 60438 Frankfurt am Main, Germany

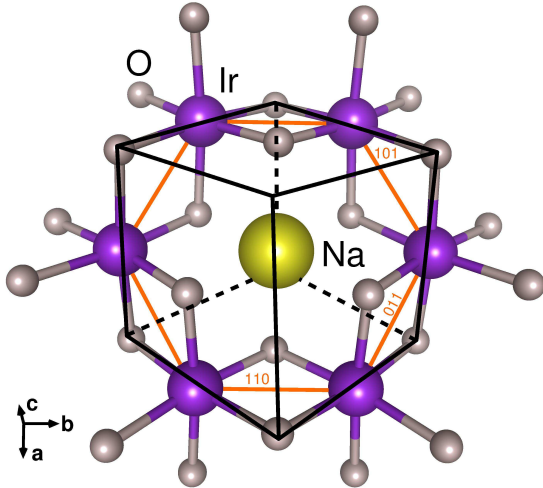
<sup>3</sup>II. Physikalisches Institut, Universität zu Köln, Zùlpicher Straße 77, 50937 Köln, Germany

(Dated: October 11, 2012)

## SUPPLEMENTARY INFORMATION

We performed density functional theory (DFT) calculations considering various full potential all electron codes, such as WIEN2k [1], ELK [2], and FPLO [3] using the generalized gradient approximation functional in its PBE form [4], and verified that the results agree reasonably well among different codes. Such comparison is particularly important because the codes implement the spin-orbit coupling in slightly different ways, employing usually unimportant, but in principle unequal approximations. In the *non-relativistic* calculations the core electrons were treated fully relativistically and the valence electrons non-relativistically (scalar relativistic approximation). In the *fully relativistic* calculations, *i.e.* with inclusion of spin-orbit coupling, all electrons were treated fully relativistically. We considered the C2/m crystal structure as given in Ref. 5 and shown in Fig. S1.

FIG. S1. Crystal structure of Na<sub>2</sub>IrO<sub>3</sub> in the cubic setting. The hexagonal direction is along the [111] direction in this setting. Ir, O and Na atoms are shown as grey, magenta, and yellow spheres, respectively. The three inequivalent Ir-Ir bonds are labeled according to their cubic directions.



We used projective Wannier functions as implemented in the FPLO basis [6] to determine a tight-binding (TB) representation for the Ir 5*d* bands. In Figure S2 we show the DFT band structure together with the bands cor-

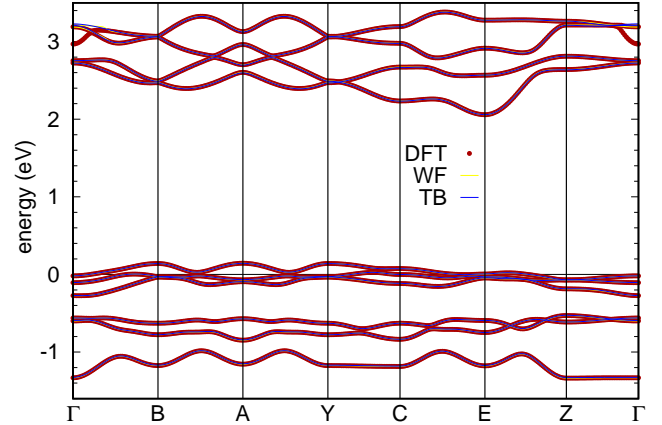


FIG. S2. Non-relativistic non-magnetic band structure of Na<sub>2</sub>IrO<sub>3</sub> (red symbols) shown together with the Wannier bands (yellow) and the tight-binding bands (blue).

responding to the Wannier representation and the TB bands derived from this representation.

In Fig. S3 we present the projective Wannier functions for the 5*d* orbitals of one Ir site. The Wannier functions exhibit the typical shape of the 5*d* functions at the Ir site. Besides, they show a clear asymmetry due to Na as well as tails on the O sites.

In order to analyze the contribution to the non-relativistic band structure of the various tight-binding hopping parameters and its relation to the quasi-molecular orbital (QMO) picture, we present in Fig. S4 the band structure that results if we restrict the tight-binding Hamiltonian to first neighbors (top left), up to second nearest neighbors (top right), up to third nearest neighbors (bottom left), and without restriction (bottom right). One can see that already the second neighbors model provides a good semiquantitative description of the band formation.

In the next Figure S5 we show the tight-binding band structures within the QMO model. In these calculations we have included the on-site trigonal splitting (the top left panel), adding the nearest neighbors  $t'_1$  hopping (top right), then the second nearest neighbors  $t'_2$  hopping (bottom left) and, finally, including also the third nearest neighbors hopping between the like orbital, which also proceeds through Na and does not take an electron out of the corresponding QMO (bottom right). The small dispersion that arises for nearest neighbors is due to devia-

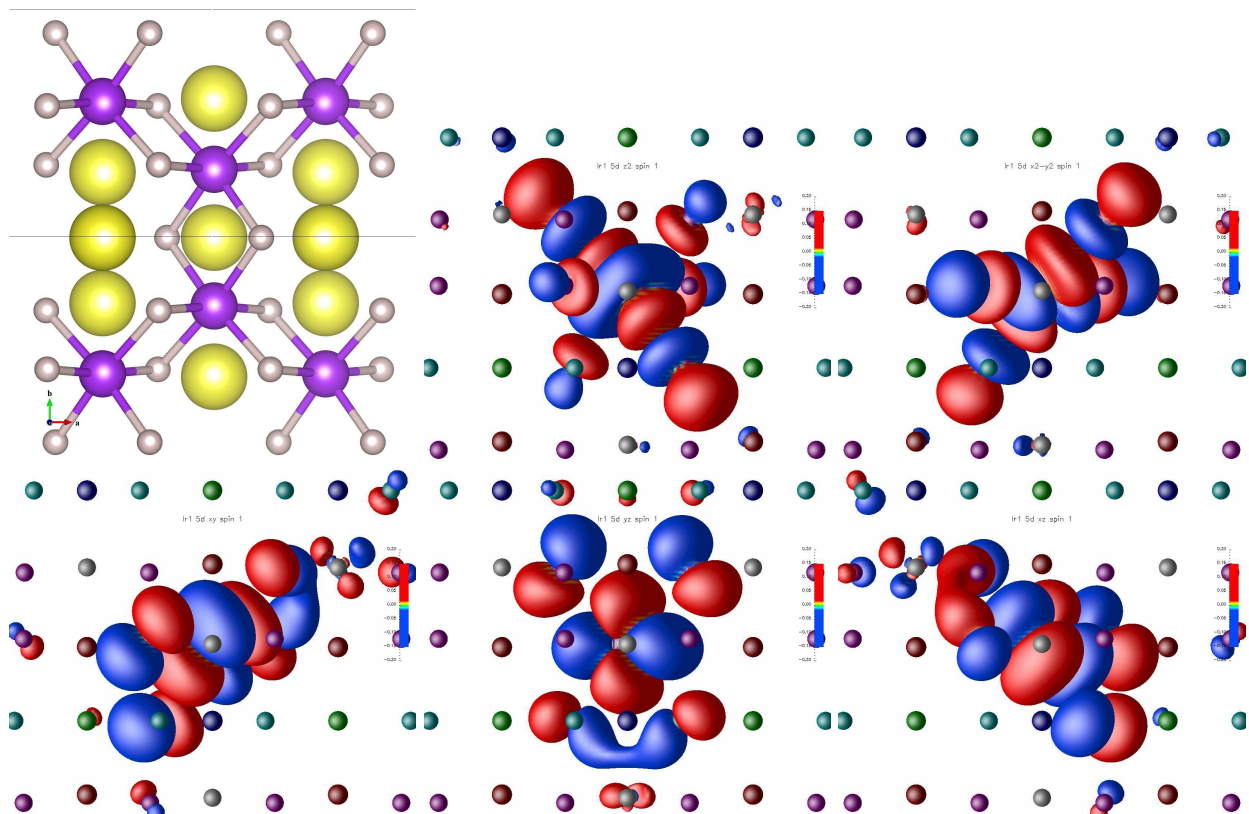


FIG. S3. Projective Wannier functions for five of the ten Ir 5d bands, together with a structure showing the perspective.

tions from the perfect octahedral environment of iridium. Upon inclusion of second nearest neighbors, as mentioned in the main text, the upper doublet and singlet merge to form one three-band manifold.

In Figure S6, we show projections of the total density of states of  $\text{Na}_2\text{IrO}_3$  onto the quasi-molecular orbitals specified in Table [1] of the main text. The eigenvector matrix

$$U = \begin{pmatrix} 1 & 1 & 1 & 1 & 1 & 1 \\ 1 & \omega & \omega^2 & -1 & \omega^4 & \omega^5 \\ 1 & \omega^5 & \omega^4 & -1 & \omega^2 & \omega \\ 1 & \omega^2 & \omega^4 & 1 & \omega^2 & \omega^4 \\ 1 & \omega^4 & \omega^2 & 1 & \omega^4 & \omega^2 \\ 1 & -1 & 1 & -1 & 1 & -1 \end{pmatrix}$$

(with  $\omega = \exp(i\pi/3)$ ) is a unitary transformation that rotates the atomic Ir  $t_{2g}$  orbitals into the QMO orbital space.  $E_{1g}$  and  $E_{2u}$  states are perfectly degenerate in the nonrelativistic case (Figure S6 (a)). When spin-orbit coupling is turned on (Figure S6 (b)), interestingly, the three upper bands are no more equivalent in this sense, with the central band being mostly  $A_{1g}$ , and the other two mostly  $E_{2u}$ . Importantly, there is hardly any mixing between the lower three bands and the upper three bands, emphasizing the fact that the low-energy physics is nearly exclusively defined by the upper three QMOs, and their mutual interaction, whether with or without spin-orbit.

At the same time, one can, alternatively, project the same bands onto the relativistic orbitals,  $j_{eff} = 1/2$  and  $j_{eff} = 3/2$ , and, as observed before[7], the upper two bands have more  $j_{eff} = 1/2$  character than  $j_{eff} = 3/2$  character. However, “more  $j_{eff} = 1/2$  character” in this context is by far not the same as “exclusively  $j_{eff} = 1/2$  character”; the overlap between the wave function of the highest band at  $\Gamma$  with the  $j_{eff} = 1/2$ ,  $\langle MO | j_{eff} = 1/2 \rangle$ , upon switching on the SO interaction, increases from  $1/\sqrt{6} \approx 0.41$  to  $\approx 0.62$ . Thus, even though the SO effects are considerable, they are not strong enough to reduce the problem to a two  $j_{eff} = 1/2$  model.

The magnetic patterns considered in our non-relativistic and fully relativistic calculations are shown in Fig. S7.

The ferromagnetic state shows in the absence of SO an energy gain of nearly 80 meV per Ir with respect to the non-magnetic solution and about half this value against competing antiferromagnetic states (zigzag and stripy phases); the simple Néel state is much higher in energy. Inclusion of SO changes the energetics considerably, as described in the main text, with the zigzag antiferromagnetic ordering becoming competitive with the ferromagnetic one, and lower in energy than the stripy phase. We deliberately do not discuss the calculated energies in detail, because the energy differences involved are on the order of one meV per atom, which is beyond

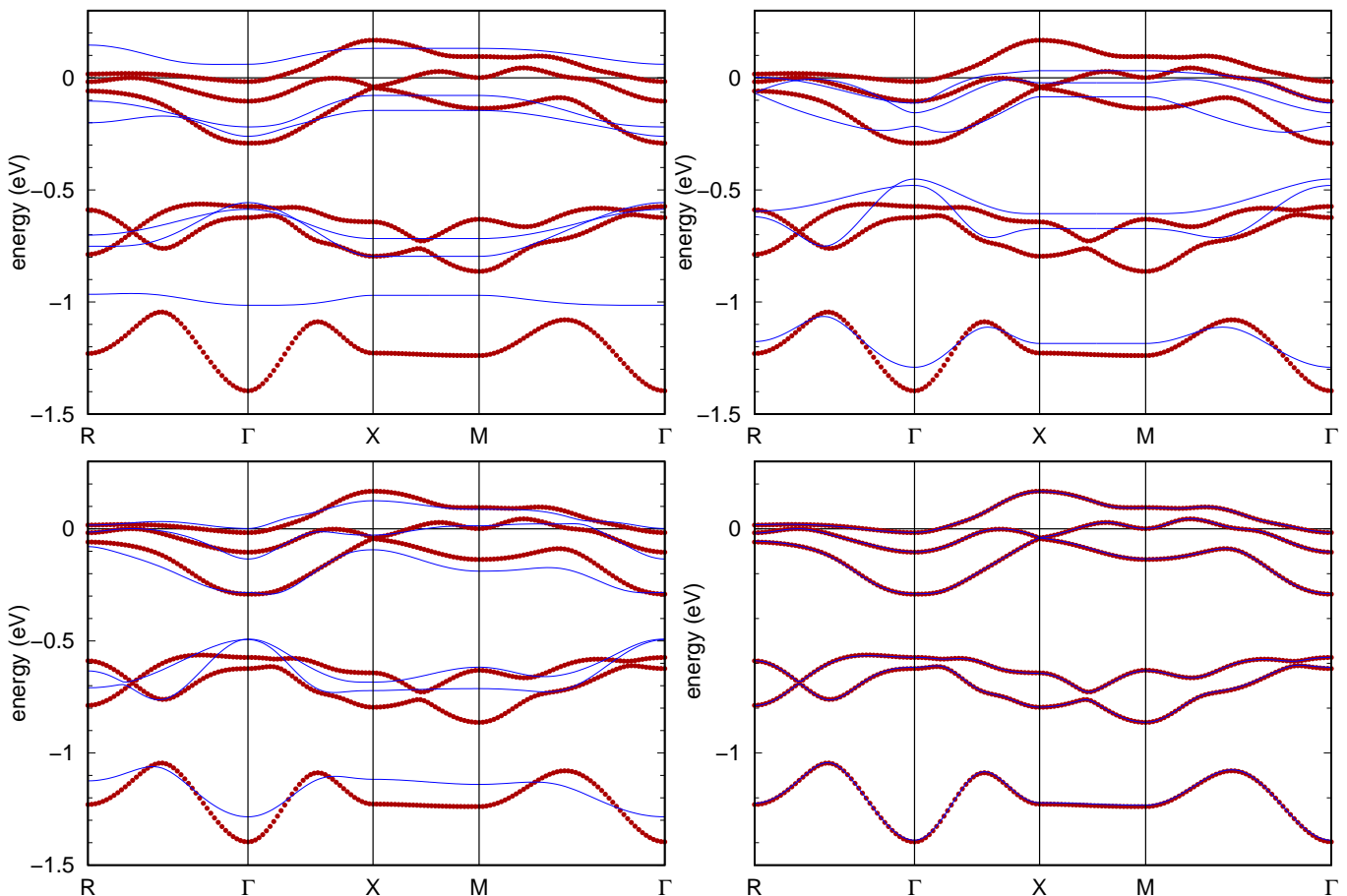


FIG. S4. Band structure of  $\text{Na}_2\text{IrO}_3$  (red symbols) shown together with the tight-binding models that include only nearest neighbors (top left), up to next nearest neighbors (top right), up to third nearest neighbors (bottom left) and neighbors up to 16 Å (bottom right).

the accuracy of the density functional theory itself, and on the border of the technical accuracy of existing band structure codes.

In Fig. S8 we show the density of states for some magnetic orderings considered in our fully relativistic calculations. Note that the zigzag ordering preserves the non-magnetic pseudogap at the Fermi level, while the stripy ordering destroys it.

Finally some considerations about the Hubbard  $U$  are at place. In fact, there are two ways of defining  $U$  in this case. As usually, the actual value of  $U$  depends on which orbitals it is being applied to. For instance, it is well known that in Fe pnictides the appropriate value of  $U$  acting on the Wannier functions combining Fe  $d$  and As  $p$  states is more than twice smaller than that acting on actual atomic  $d$  orbitals since the screening effects change depending on the basis of active states considered. In molecular solids, such as fullerides, the atomic value of  $U$  often appears completely irrelevant, and the physically meaningful value of  $U$  is the (much smaller) energy of Coulomb repulsion of two electrons placed on two molecular orbitals. In the case of  $\text{Na}_2\text{IrO}_3$  one has a choice of

using an atomic  $U \sim 1.5\text{-}2$  eV, realizing that the results will be strongly affected by the fact that electrons are localized not on individual ions, but on individual QMOs, or of constructing  $U$  in the QMO basis. The former way is readily available in such formalisms as LDA+ $U$  but it may be a poor choice for the description of a system based on quasi-molecular orbitals.

- 
- [1] P. Blaha, K. Schwarz, G. K. H. Madsen, D. Kvasnicka, and J. Luitz 2001 WIEN2k, *An Augmented PlaneWave+LocalOrbitals Program for Calculating Crystal Properties* (Karlheinz Schwarz, Techn. Universität Wien, Austria).
  - [2] <http://elk.sourceforge.net/>
  - [3] K. Koepnik and H. Eschrig, Phys. Rev. B **59**. 1743 (1999); <http://www.FPLO.de>
  - [4] J. P. Perdew, K. Burke and M. Ernzerhof, Phys. Rev. Lett. **77** 3865 (1996).
  - [5] S. K. Choi, R. Coldea, A. N. Kolmogorov, T. Lancaster, I. I. Mazin, S. J. Blundell, P. G. Radaelli, Yogesh Singh, P. Gegenwart, K. R. Choi, S.-W. Cheong, P. J. Baker, C.

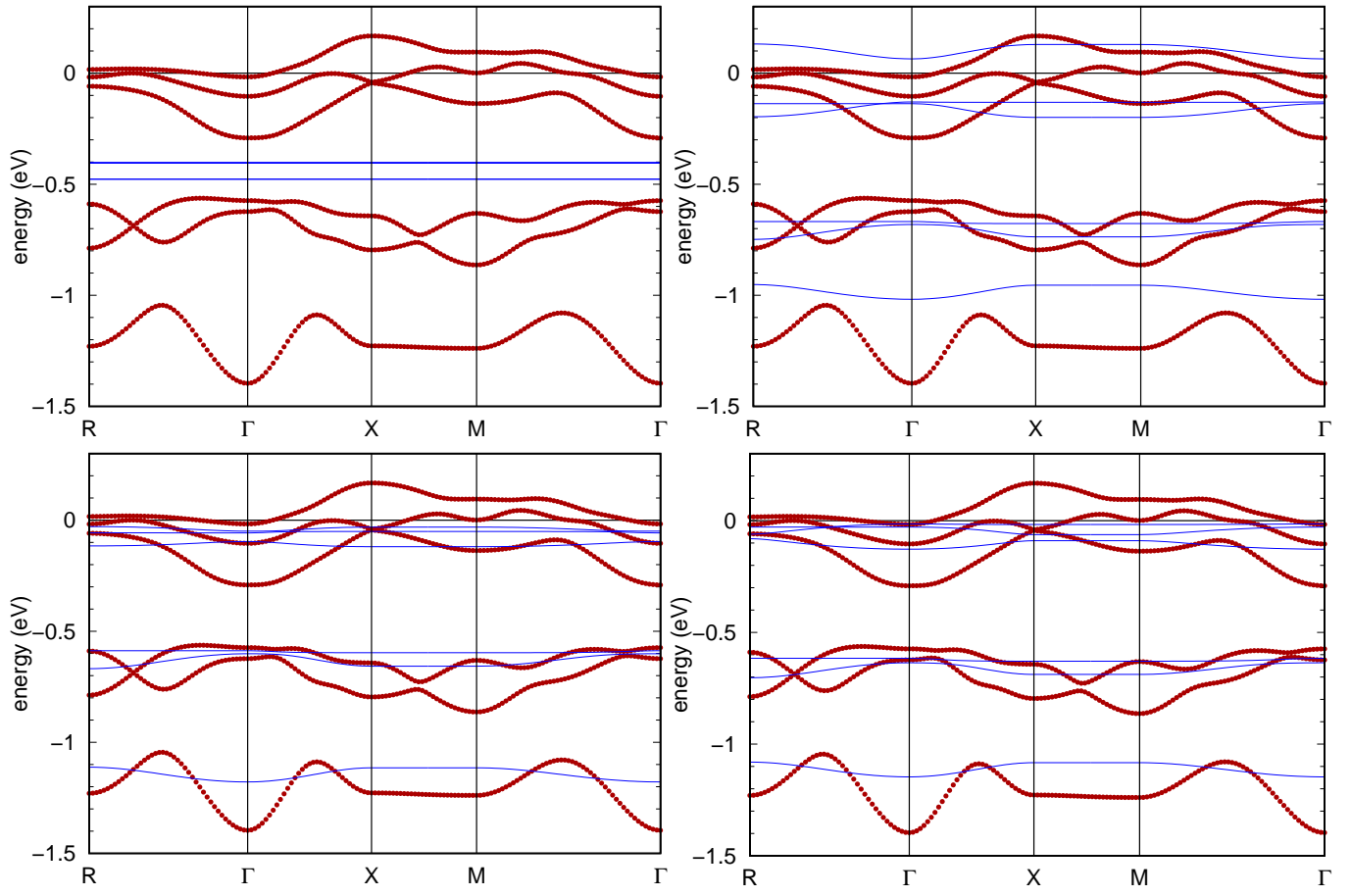


FIG. S5. Band structure of Na<sub>2</sub>IrO<sub>3</sub> (red symbols) shown together with the tight-binding models that involve only parameters compatible with the quasi-molecular orbitals. Only on-site parameters (top left), up to nearest neighbors (top right), up to second nearest neighbors (bottom left) and up to third nearest neighbors (bottom right).

Stock, J. Taylor, Phys. Rev. Lett. **108**, 127204 (2012).

[6] H. Eschrig and K. Koepf, Phys. Rev. B **80**, 104503 (2009).

[7] A. Shitade, H. Katsura, J. Kuneš, X.-L. Qi, S.-C. Zhang, and N. Nagaosa, Phys. Rev. Lett. **102**, 256403 (2009).

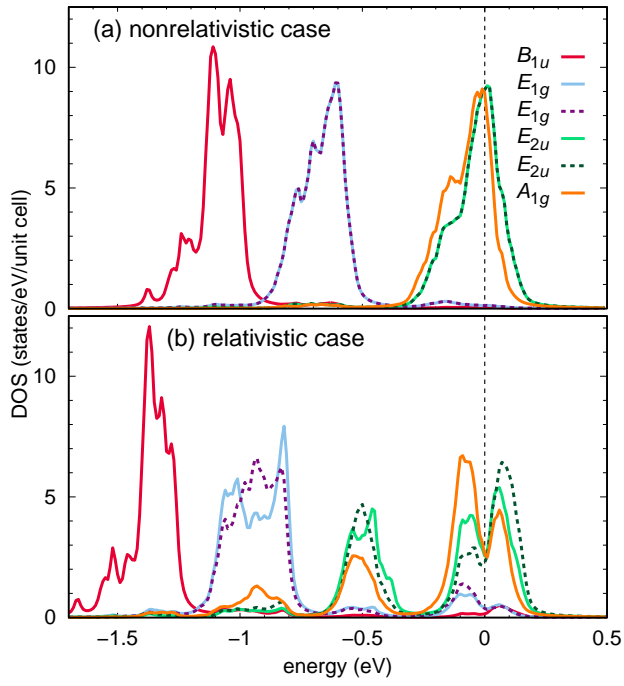


FIG. S6. Density of states of  $\text{Na}_2\text{IrO}_3$  projected onto the six quasi-molecular orbitals given in Table [1] of the main text for (a) a nonrelativistic and (b) a relativistic calculation.

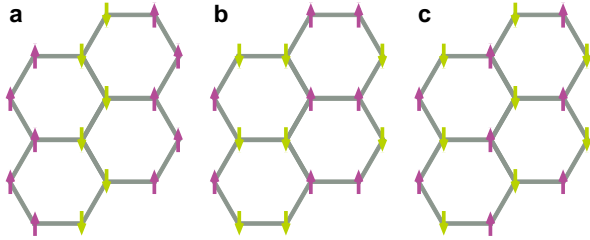


FIG. S7. Three antiferromagnetic patterns considered in this paper: (a) zigzag, (b) stripy, and (c) Néel.

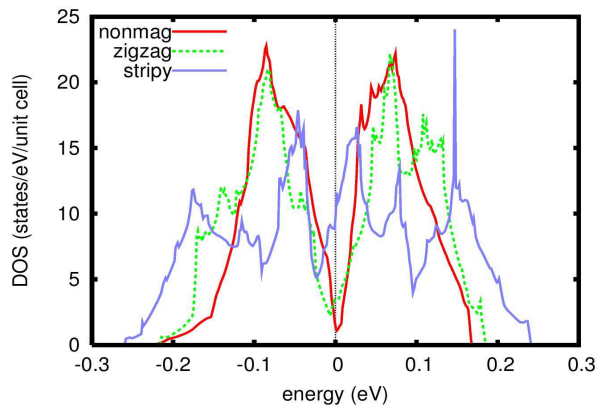


FIG. S8. Density of states, spin-orbit included, for two competing magnetic patterns compared with that for the nonmagnetic state.